View metadata, citation and similar papers at core.ac.uk
brought to you by CORE
provided by NASA Technical Reports Server

Properties, propagation, and excitation of EMIC waves observed by MMS: A case study

Jichun Zhang[1] and Victoria N. Coffey[2]
University of New Hampshire 1, Durham, NH 03824
NASA Marshall Space Flight Center 2, Huntsville, AL 35812

Michael O. Chandler[2], Scott A. Boardsen[3], Anthony A. Saikin[1], Emily M. Mello[1], Christopher T. Russell[4], Roy B. Torbert[1], Stephen A. Fuselier[5], Barbara L. Giles[3], and Daniel J. Gershman[3]
NASA Goddard Space Flight Center 3, Greenbelt, MD 20771
UCLA, Los Angeles 4, CA 951567
Southwest Research Institute 5, San Antonio, TX 78238

Abstract

Electromagnetic ion cyclotron (EMIC) waves (0.1-5 Hz) play an important role in particle dynamics in the Earth's magnetosphere. EMIC waves are preferentially excited in regions where hot anisotropic ions and cold dense plasma populations spatially overlap. While the generation region of EMIC waves is usually on or near the magnetic equatorial plane in the inner magnetosphere, EMIC waves have both equatorial and off-equator source regions on the dayside in the compressed outer magnetosphere. Using field and plasma measurements from the Magnetospheric Multiscale (MMS) mission, we perform a case study of EMIC waves and associated local plasma conditions observed on 19 October 2015. From 0315 to 0810 UT, before crossing the magnetopause into the magnetosheath, all four MMS spacecraft detected long-lasting He^+-band EMIC wave emissions around local noon (MLT = 12.7 – 14.0) at high L-shells (L = 8.8 – 15.2) and low magnetic latitudes (MLAT = -21.8º – -30.3º). Energetic (> 1 keV) and anisotropic ions were present throughout this event that was in the recovery phase of a weak geomagnetic storm (min. *Dst* = -48 nT at 1000 UT on 18 October 2015). The testing of linear theory suggests that the EMIC waves were excited locally. Although the wave event is dominated by small normal angles, its polarization is mixed with right- and left-handedness and its propagation is bi-directional with regard to the background magnetic field. The short inter-spacecraft distances (as low as ~15 km) of the MMS mission make it possible to accurately determine the k vector of the waves using the phase difference technique. Preliminary analysis finds that the k vector magnitude, phase speed, and wavelength of the 0.3-Hz wave packet at 0453:55 UT are 0.005 km^{-1}, 372.9 km/s, and 1242.9 km, respectively.

---

[1] Research Associate Professor, Department of Physics, Space Science Center, University of New Hampshire.
[2] Research Scientist, Natural Environments, EV44 Huntsville AL 35812, NASA Marshall Space Flight Center.
[3] Research Scientist, Natural Environments, EV44 Huntsville AL 35812, NASA Marshall Space Flight Center.
[4] Research Scientist, Goddard Planetary Heliophysics Institute, College Park MD 20742, University of Maryland.
[5] Graduate Student Research Assistant, Department of Physics, 8 College Road, Durham, NH 03824, Space Science Center.
[6] Research Assistant, Department of Physics, 8 College Road, Durham, NH 03824, Space Science Center.
[7] Professor, Department of Earth, Planetary, and Space Sciences, 595 Charles Young Drive East, Los Angeles, CA 90095, Institute of Geophysics and Planetary Physics.
[8] Professor, Department of Physics, 8 College Road, Durham, NH 03824, Space Science Center.
[9] Executive Director, Space Science Department, 6220 Culebra Road, San Antonio, TX 78238, Southwest Research Institute.
[10] Associate Chief, Geospace Physics Laboratory, 6730 Greenbelt MD 20771, NASA Goddard Space Flight Center.
[11] Research Scientist, Goddard Planetary Heliophysics Institute, College Park MD 20742, University of Maryland.

I. Introduction

Electromagnetic ion cyclotron (EMIC) waves, typically in the frequency range of 0.1-5 Hz, are called Pc 1-2 pulsations when seen on the ground. They are normally excited by a temperature anisotropic ($T_\perp > T_\parallel$) distribution of hot (~1-100 keV) ions. [2-4] Under a dipole-like magnetic field configuration in the Earth's inner magnetosphere (see Fig. 1), the excitation region of EMIC waves is usually on or near the magnetic equatorial plane, [5, 6] where the magnetic energy per particle is lower and thus the growth rate of waves is larger due to the greater plasma density and weaker magnetic field strength. [2] EMIC waves are preferentially generated in regions where hot anisotropic ions and cold dense plasma populations spatially overlap (Fig. 2). [7-10] In the terrestrial inner magnetosphere, these ion populations can commonly be found where the ring current overlaps the outer plasmasphere and plasmapause [4, 11, 12] and the "edges" of plasmaspheric drainage plumes. [5, 13, 14] A significant population of hot anisotropic H^+ can also be created on the dayside outer magnetosphere through the drift-shell splitting, [15, 16] the Shabansky orbits (a non-energization mechanism), [17, 18] or during a magnetospheric compression, which is often driven by a sudden, large increase in the solar wind dynamic pressure (*Pdyn*). [19-23] Because of the dayside geomagnetic field compression in the outer magnetosphere by *Pdyn*, local minimum *B* regions can be formed off the magnetic equator in the dayside magnetosphere (see Fig. 2). [1] EMIC waves excited near the off-equator minimum *B* regions have been investigated in recent theoretical work, [18, 23] followed by observational evidence. [24-26] Due to the distortion of the geomagnetic field from a simple dipole field and the spatial extent of EMIC wave source regions, EMIC waves and the associated plasma conditions have not been fully understood in the outer magnetosphere.

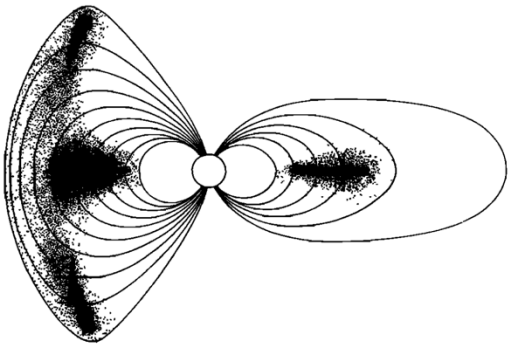

Figure 1. Schematic sketch of chorus/EMIC wave excitation regions, denoted by dots, on the noon-midnight meridian plane. [1]

As displayed in the lower part of Fig. 2, the excited EMIC waves can result in the energization and loss of magnetospheric particles. [2, 27-30] Through resonant wave-particle interactions, EMIC waves are able to accelerate cold ions into the thermal (~1eV – 1 keV) energy range in the direction perpendicular to the ambient magnetic field [27-29, 31, 32] and cause the pitch angle scattering loss of hot ions in the ring current. [33-35] Particularly, previous studies [30, 36-47] have confirmed that EMIC waves can also resonantly interact with relativistic electrons and result in pitch angle scattering of the electrons.

Newly excited EMIC waves are often transverse and left-hand polarized, consistent with the direction of ion gyration in the magnetic field. [2] After being generated, EMIC waves can be guided along the magnetic field lines and propagate from the source region to other magnetic latitudes (MLATs). In the case of the equatorial source region, they propagate from the equatorial plane to higher MLATs. Using the Combined Release and Radiation Effects Satellite (CRRES) electric and magnetic field data (covering only MLT = 1400 – 1800), *Loto'aniu et al.* [6] found that the directions of the energy propagation (i.e., Poynting vector) of EMIC waves are unidirectional when |MLAT| > 11° but they are bidirectional in the MLAT range of [-11°, 11°] in the inner magnetosphere. *Khazanov et al.* [48] claimed that most unidirectional events were indeed detected beyond the range of MLAT = [-18°**,** 18°**]** due to data gaps in the statistical study by *Loto'aniu et al.* [6] Depending on their frequency with respect to the local ion gyrofrequencies such as f_{He+}, some waves are well guided along the field lines and can generally propagate to the ground. [49] Some waves may even experience a polarization reversal where the wave frequency *f* is equal to the crossover frequency f_{co} during their higher-latitude propagation and then be reflected where *f* equals the bi-ion hybrid frequency f_{bi} at an even higher latitude. [49] As a result, their polarization is crossed over from a left-hand to a right-

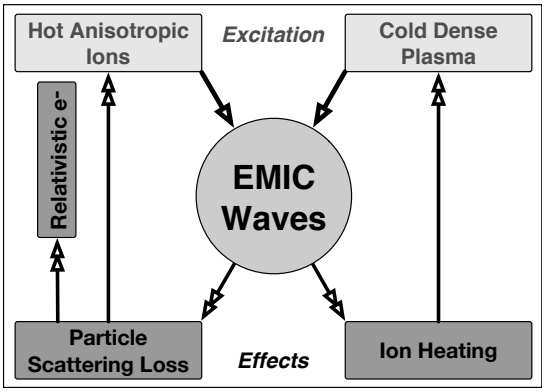

Figure 2. A schematic diagram depicting the excitation and effects of EMIC waves. The overlapping of hot anisotropic ions and cold dense plasma result in the generation of EMIC waves, and EMIC waves in turn cause the ion heating of the cold dense plasma and the pitch angle scattering of both relativistic electrons (e^-) and hot ions through resonant wave-particle interactions.

hand or linear mode. These waves could undergo multiple equatorial crossings along magnetic flux tubes without a large radial or azimuthal drift. Because of their successive passes through the equatorial wave growth region, the waves are expected to be drastically amplified by continuing to obtain energy from the energetic protons. [49, 50] Nevertheless, *Horne and Thorne* [51] found that, in the absence of density gradients, significant wave amplifications can only occur on the first equatorial pass because wave normal angles become large after the initial pass. *Horne and Thorne* [52] concluded that wave damping by thermal heavy ions also makes it impossible for the same EMIC wave packet to bounce through its source region multiple times. But, a consensus about the wave propagation and reflection has not been reached. [48, 50, 53]

In this study, using *in situ* field and plasma measurements from the Magnetospheric Multiscale (MMS) mission, we perform a case study of EMIC waves and associated local plasma conditions in the outer magnetosphere on 19 October 2015. The concentration of our current work is on the wave properties, propagation, excitation, and the calculation of wave **k** vector at one time point. The current investigation is also a follow-up to our recently published case and statistical studies of EMIC waves detected by Van Allen Probes [4, 54-56] in the inner magnetosphere and by Cluster [26, 28, 57-59] in a polar orbit.

This paper is organized as follows: after the introduction (current section), we describe MMS instrumentation in Section 2. Section 3 presents results from the case study of the EMIC wave event. Conclusions and future work are discussed in Section 4.

II. MMS Instrumentation

The MMS mission [60] has four identical spacecraft, which were launched into 24-hour period, highly elliptical, near-equatorial orbits on 12 March 2015. The MMS spacecraft are positioned in a tetrahedron formation of variable inter-spacecraft distances from tens to hundreds of kilometers. Multiple instruments onboard each MMS spacecraft measure and derive a variety of parameters from plasma particles and magnetic and electric fields.

In this study, the high-resolution field measurements are used to obtain wave frequency spectrums utilizing the Fast Fourier Transform (FFT) technique. Magnetic field (8 or 15 Hz) and electric field (33 Hz) data are obtained from the Fluxgate Magnetometers (FGMs) [61] and the spin-plane double-probe electric-field sensors (EDPs) in the FIELDS instrument suite, respectively. [62] MMS FIELDS includes a sensor suite consisting of two axial and four spin-plane double-probe electric-field sensors, two flux-gate magnetometers, a search-coil magnetometer, and two electron drift instruments onboard each MMS spacecraft. These instruments measure the DC magnetic field with a resolution of 10 ms, the DC electric field with a resolution of 1 ms, electric plasma waves to 100 kHz, and magnetic plasma waves to 6 kHz.

Plasma data are from the Fast Plasma Investigation (FPI) [63] and the Hot Plasma

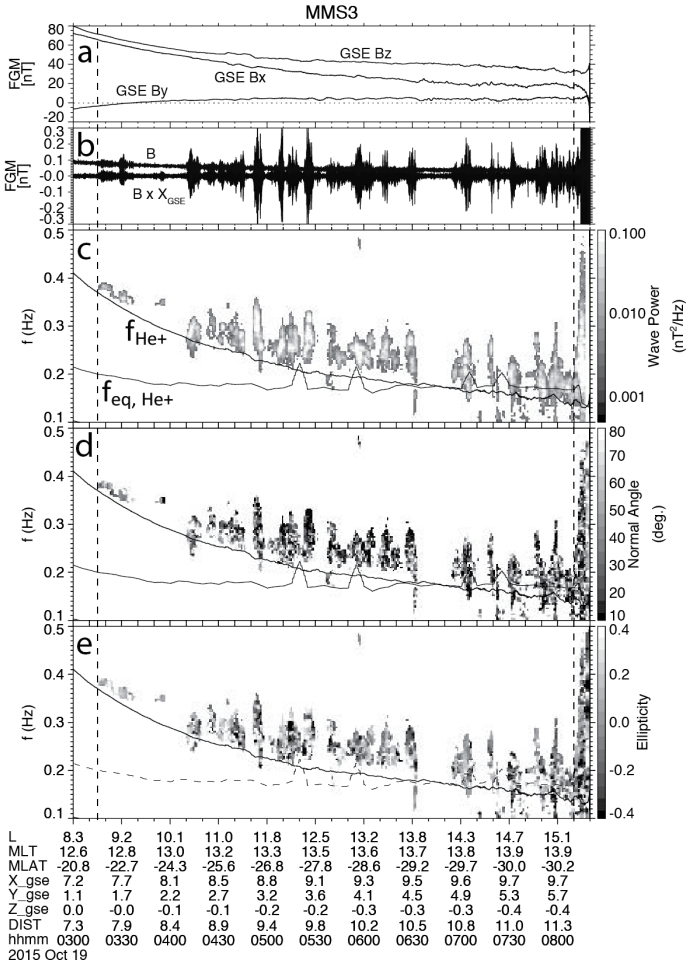

Figure 3. (a) Three measured high-resolution magnetic field components in the geocentric solar ecliptic (GSE) coordinates, (b) waveforms in the field-aligned coordinates (FAC) after the ambient magnetic field is filtered out, and (c) frequency-UT spectrograms of wave power, (d) normal angle, and (e) ellipticity (<0, L-mode; >0, R-mode). The vertical dashed lines indicate the start and end times of the wave event. The solid/dashed traces in Panels c-e represent local/equatorial He^+ gyrofrequencies $f_{He+}/f_{eq,He+}$.

Composition Analyzer (HPCA). [64] FPI includes four dual electron spectrometers (DES) and four dual ion spectrometers (DIS) on each of the four spacecraft. When measurements from the two sets of four dual-spectrometers are combined, FPI can provide the velocity-space distribution of electrons and ions from 10 eV to 30 keV with a time resolution of 30 and 150 ms, respectively. One HPCA on each spacecraft measures the composition-resolved velocity-space distribution of ions from 1 eV to 40 keV with a time resolution of 10–15 s.

III. EMIC wave event on 19 October 2015

A. Field Data and Wave Activity

Figure 3 demonstrates high-resolution magnetic field data measured by MMS/FGM from 0300 to 0820 UT on 19 October 2015 and their results from the FFT analysis, using 1024 time points and a step length of 32 points. The magnetic field data are first converted into field-aligned coordinates (FAC) and then the FFT spectral analysis [65] is applied to obtain waveforms, wave power, normal angle, and ellipticity (<0, L-mode; >0, R-mode) for the EMIC wave event. When wave powers (Fig. 3c) are less than 0.002 nT^2/Hz, data points are removed from the spectrogram plots shown in Figs. 3c-e. The EMIC wave event is labeled with the two vertical dashed lines, starting at 0315 and lasting for 4 hours 55 minutes. The event exhibits multiple shorter-period wave activity in the frequency ranges mostly above f_{He+}, i.e., in the H^+ band. The wave event is dominated by small normal angles, and its polarization is mixed with right- and left-handedness. All four MMS spacecraft detected the long-lasting EMIC wave emissions in the same UT time period. The EMIC waves were around local noon (MLT = 12.7 – 14.0), at high L-shells (L = 8.8 – 15.2), and at low magnetic latitudes (MLAT = -21.8 – -30.3°).

Figure 4 shows the X and Y components of wave electric and magnetic fields, the Z component of wave Poynting vector spectrograms (S_z), and angles (*AngBS*) between the background magnetic field and the Poynting vector on MMS3 during the EMIC wave event. We obtain the waveform data by applying a 0.1- to 0.5-Hz band-pass filter to both the *in situ* FGM magnetic field measurements and EDP electric field measurements, after they are transferred into the local field-aligned coordinate system. The transverse (i.e., X and Y) components of electric and magnetic fields are used to compute S_z with the following formula: [6]

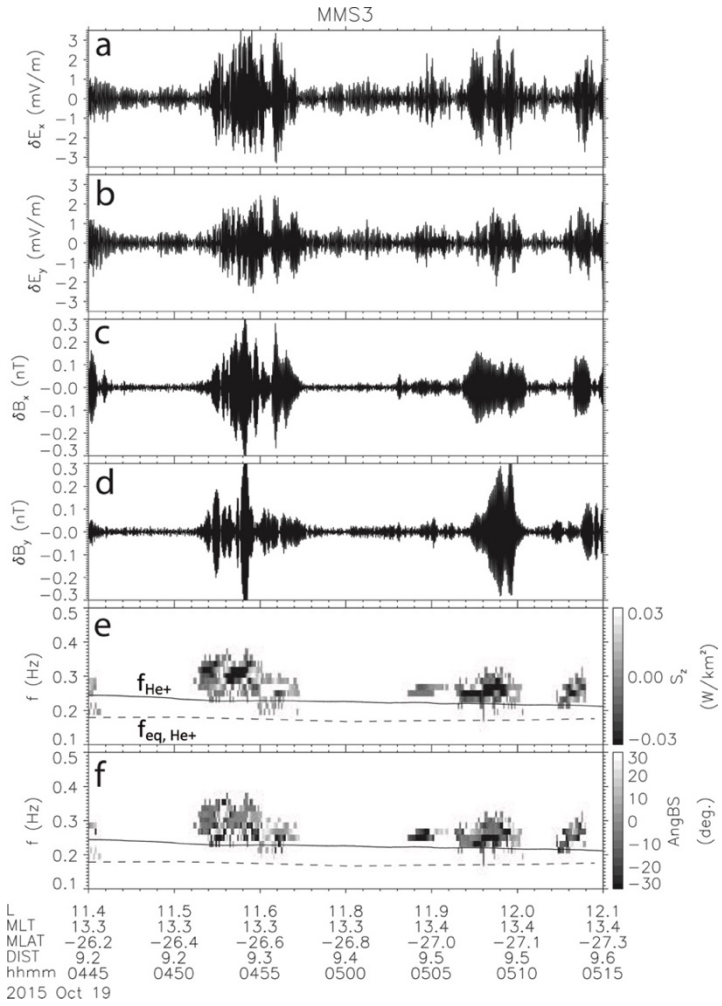

Figure 4. Wave fields and Poynting vector on MMS3 during 0445 – 0515 UT, 19 October 2015. From top to bottom, the panels show wave electric field components (δE_x and δE_y), wave magnetic field components (δB_x and δB_y), Poynting vector Z component (S_z), and the angles (*AngBS*) of the background magnetic field and the Poynting vector. The data are transferred into the local field-aligned coordinate system: Z is along the magnetic field, $Y=Z\times X_{GSE}$, and $X=Y\times Z$, which completes the right-hand system. The solid/dashed traces in Panels e-f represent the local/equatorial He^+ gyrofrequencies $f_{He+}/f_{eq,He+}$.

$$\mathbf{S} = \frac{1}{4\mu}(\delta\mathbf{E}^* \times \delta\mathbf{B} + \delta\mathbf{E} \times \delta\mathbf{B}^*) \quad (1)$$

where **S** is the wave Poynting vector spectrograms, **δE** and **δB** are the complex spectral matrices of the wave fields, and **δE*** and **δB*** are their conjugate matrices. The wave Poynting vector points the propagation direction of the wave energy, same as that of the wave group velocity $\mathbf{V_g}$. In the event, the peak value of δE_x (δE_y) is 3.5 (-2.6) mV/m, and the maximum magnitude of δB_x and δB_y is 0.3 (0.3) nT. To highlight the sign change in S_z, S_z is plotted in a narrow range, i.e., [-0.03, 0.03] W/km^2, and all its values are marked as NaN when they are $\leq 3\times10^{-4}$ W/km^2. The minimum (maximum) value of S_z is -0.25 (1.19) W/km^2 during the plotting period. The energy propagation of the EMIC waves is bi-directional with regard to the ambient magnetic field. This indicates the local excitation of the wave activity. Later in the paper, we will further test whether local plasma conditions are associated with the generation of the waves.

B. Solar Wind and Geomagnetic Conditions

From top to bottom, Fig. 5 shows the solar wind bulk flow speed *Vsw*, plasma number density *Nsw*, dynamic pressure *Pdyn*, interplanetary magnetic field (IMF) magnitude *B*, IMF z-component B_z, *AE, Kp*, and *Dst* and *Dst** (in the same panel), respectively. The plotting time period is 3.5 days from 0000 UT, 17 October 2015. *Dst** is the *Pdyn*-corrected *Dst*, which does not include the contribution of the magnetopause currents to disturbances in the geomagnetic field. $Dst^*=Dst-7.26Pdyn^{1/2}+11$ nT. [66] The solar wind plasma/IMF data are in 1-minute resolution and obtained from the High Resolution OMNI (HRO) database, which is contained in NASA/GSFC's Space Physics Data Facility's OMNIWeb service. This service provides solar wind data propagated to the Earth's bow shock nose using the minimum variance analysis (MVA) technique. [67-69] Similar to Fig. 3, the vertical dashed lines indicate the duration of the EMIC wave event.

The EMIC wave event occurred in the middle recovery phase of a moderate geomagnetic storm that has maximum *AE* = 1400, maximum *Kp* = 4, and minimum *Dst** = -51.5 nT at 0900 UT, 18 October 2015. The minimum *Dst** is denoted with the vertical dotted line in Fig. 5. The intensity of the storm is consistent with the levels of disturbances in solar wind plasma and IMF, particularly the magnitude and duration of the southward IMF B_z.

C. Plasma Observations and Comparison with Linear Theory

To quantitatively evaluate conditions for the excitation of the EMIC waves, we test the linear theory of the EMIC instability with local

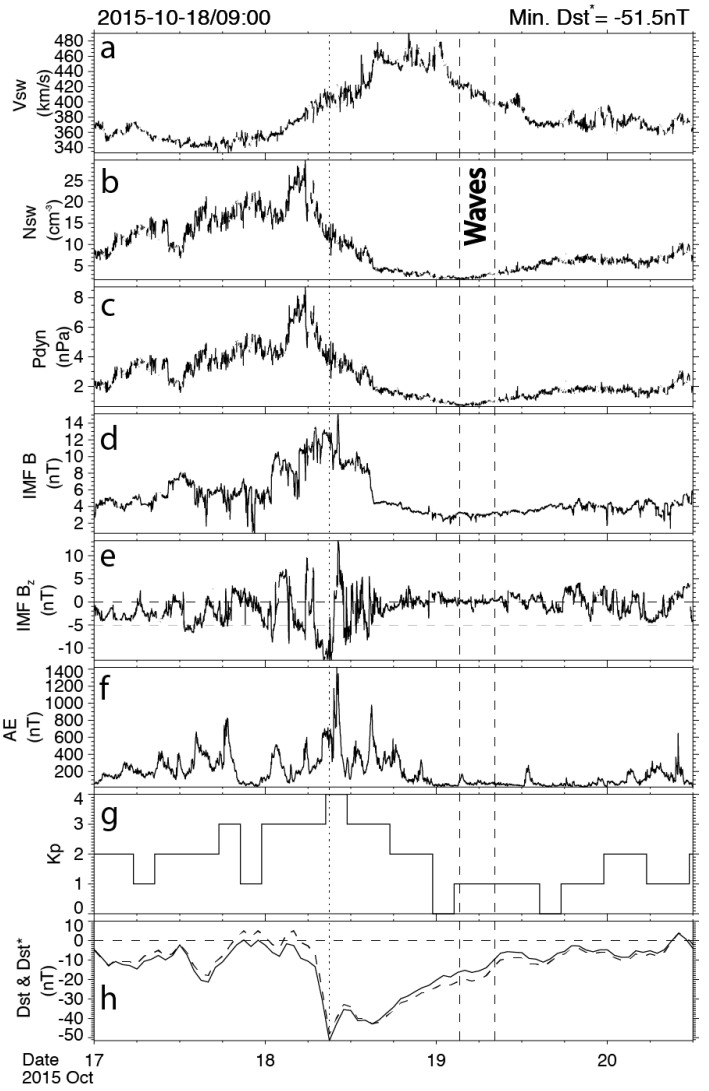

Figure 5. Solar wind plasma, IMF, and geomagnetic indices during the EMIC wave event: 0000 UT, 17 October to 1200 UT, 20 October 2015. Shown from top to bottom are solar wind bulk flow speed *Vsw*, plasma number density *Nsw*, dynamic pressure *Pdyn*, IMF *B*, IMF B_z, *AE*, *Kp*, and *Dst overplotted with *Dst*. The vertical dashed lines indicate the time periods of the wave activity, and the vertical dotted lines denote the time of min. *Dst**. In (e), the horizontal dashed lines indicate the values of 0 and −5 nT, respectively. In (h), the horizontal dashed lines mark the zero value.**

magnetic field and plasma parameters, which are derived from the H^+ energy and pitch angle (PA) fluxes. Based on linear theory, EMIC wave activity can occur only if $\Sigma_h > S_h$. [70] S_h is the EMIC instability threshold,

$$S_h = \sigma_0 + \sigma_1 \ln(\frac{n_{hp}}{n_e}) + \sigma_2 [\ln(\frac{n_{hp}}{n_e})]^2, \quad (2)$$

where σ_0 = 0.429, σ_1 = 0.124, and σ_2 = 0.0118. These constants are given in Ref. 71, obtained by assuming the wave growth rate is 0.001 and fitting linear theory results to LANL Magnetospheric Plasma Analyzer (MPA) observations at geosynchronous orbit. n_{hp} ("hp" denotes hot protons) is the density of hot (e.g., >1 keV) H^+ and n_e is the total electron density. Σ_h is the observational EMIC growth parameter,

$$\Sigma_h = (\frac{T_\perp}{T_\parallel} - 1)\beta_{\parallel h}^{\alpha_h}, \quad (3)$$

where

$$\beta_{\parallel h} = 2\mu_0 n_{hp} k T_\parallel / B^2 \quad (4)$$

$$\alpha_h = a_0 - a_1 \ln(\frac{n_{hp}}{n_e}) - a_2 [\ln(\frac{n_{hp}}{n_e})]^2 \quad (5)$$

and a_0 = 0.409, a_1 = 0.0145, and a_2 = 0.00028. [71] $T_\perp$ ($T_\parallel$) is the temperature perpendicular (parallel) to the background magnetic field, $T_\perp / T_\parallel - 1$ is the temperature anisotropy, and B is the magnetic field magnitude.

MMS measured the plasma and magnetic field parameters for the EMIC wave event, which allows us to test the threshold of the EMIC instability for the observed conditions. Fig. 6 shows several associated parameters from MMS3 from 0240 – 0845 UT on 19 October 2015: HPI-DIS ion flux spectrograms, HPCA H^+ flux spectrograms, temperature anisotropy for >1 keV H^+, $A_{hp} = T_\perp / T_\parallel - 1$, n_{hp} for >1 keV H^+, n_e, $|B|$, $\beta_{\parallel h}$ for >1 keV H^+, Σ_h, S_h, and the difference between Σ_h and S_h. The H^+ moments ($T_\perp$, $T_\parallel$, and n_{hp}) are calculated with H^+ 3-D distributions measured by HPCA over all energy channels. Again, the start and end time of the wave events are denoted

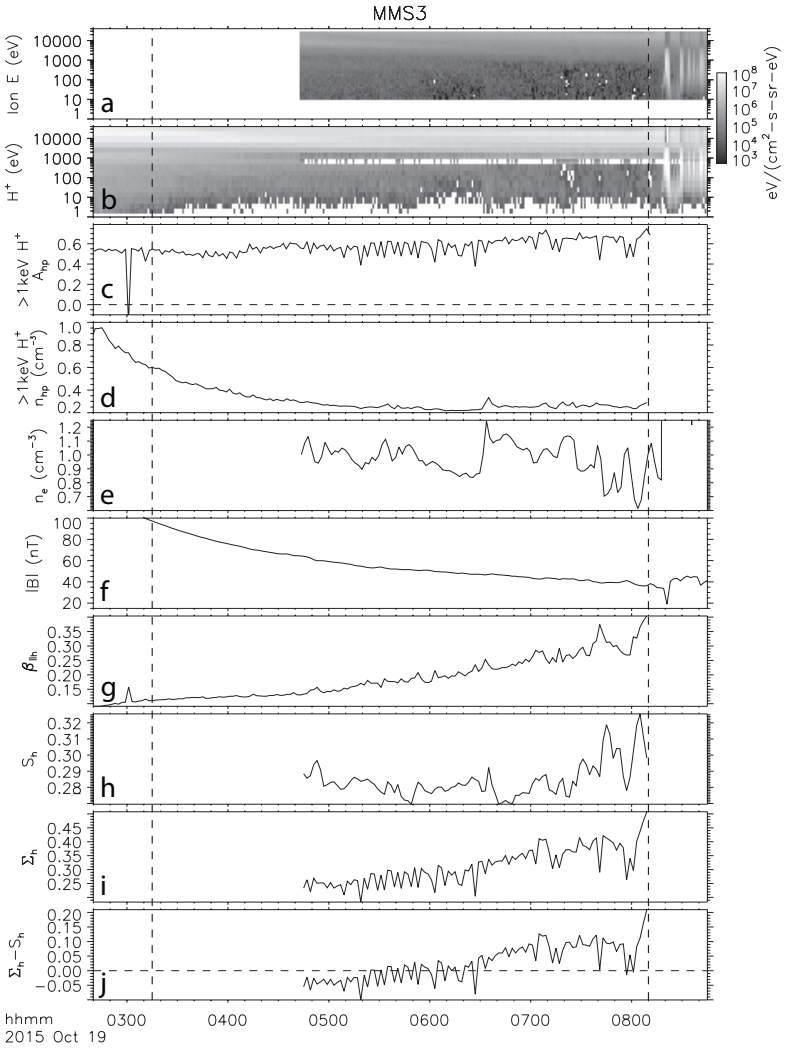

Figure 6. EMIC instability related parameters on MMS3 from 0240 – 0845 UT on 19 October 2015. From top to bottom, the panels show HPI-DIS ion energy-UT flux spectrograms, HPCA H^+ energy-UT flux spectrograms, hot-proton (>1 keV) temperature anisotropy ($A_{hp} = T_\perp / T_\parallel - 1$), hot-proton density ($n_{hp}$), electron density ($n_e$), magnetic field magnitude ($|B|$), hot-proton parallel plasma beta ($\beta_{\parallel h}$), the observational EMIC wave growth parameter (Σ_h), the theoretical EMIC instability parameter (S_h), and their difference ($\Sigma_h - S_h$). The vertical dashed lines indicate the start and end times of the wave event. In Figs. 6c and 6j, the horizontal dashed line marks the value of 0.

by the pair of the vertical dashed lines. In Figs. 6c-6j, the critical value of zero is marked with the horizontal dashed lines. n_e is the total electron density by DES with a multiplication factor of 1.2 (suggested by S. A. Boardsen). This factor is estimated by comparing the difference between the measured total DES n_e and electron density derived from the frequencies of MMS-detected upper hybrid waves.

As shown in Figs. 6a-6b, energetic (> 1 keV) ions are present throughout the EMIC wave event. A_{hp} is moderately high during the wave event, with the maximum average value at 0.75. The n_{hp} average is ~0.3 cm^{-3} during the periods of the waves. The wave event occurred at low MLATs, close to local minimum $|B|$ regions (i.e., on the magnetic equatorial plane). The average of $|B|$ is ~60 nT. In contrast to n_{hp} and $|B|$, $\beta_{\|h}$ keeps increasing from the beginning of the wave event, peaking at 0.4 in the end. While Σ_h -S_h (varying as Σ_h) is not always >0 during the EMIC wave activity, the average of Σ_h -S_h exceeds 0 and is clearly elevated closer to the end of the wave event. It reaches a positive value as high as 0.22 in the end.

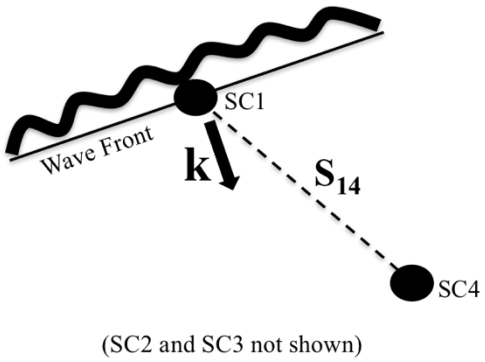

Figure 7. A schematic diagram of the EMIC wave packet at ~0453:55 UT on 19 October 2015, which arrived first at SC1 and then at the other three spacecraft (only SC4 shown) at later times.

D. Wave k Vector

As long as the spatial configuration of the four MMS spacecraft is such that the so-called "spatial aliasing" [72] can be avoided, multipoint measurements of the spacecraft can make it possible to determine wave vector **k**.[73-76] For instance, using high-resolution EDP electric field measurements from the four MMS spacecraft during the 19 October 2015 event, we can determine **k** and thus several other important wave parameters of the wave activity. [76] Figure 7 illustrates the arrival of the EMIC wave packet (f = 0.3 Hz) at ~0453:55 UT first at MMS1 (SC1) and then at MMS2 (SC2), MMS4 (SC4), and MMS3 (SC3) with a time delay of 0.031 s (dt_{12}), 0.047 s (dt_{14}), and 0.054 s (dt_{13}), respectively. The wave phase velocity $\mathbf{V_p}$ can be found by solving

$$\mathbf{S_{1i}} \cdot \frac{\mathbf{V_p}}{{V_p}^2} = dt_{1i} \qquad (6)$$

where i = 2, 3, and 4 and $\mathbf{S_{1i}}$ is the distance vector between SC1 and the other spacecraft. In the geocentric solar ecliptic (GSE) coordinates, $\mathbf{V_p}$ = (43.3, 360.8, 83.3) km/s. Therefore, the wavelength $\lambda = \mathbf{S_{1i}} \cdot \mathbf{n_{v_p}}/(f dt_{1i})$ = 1242.9 km, $|\mathbf{k}| = 2\pi/\lambda$ = 0.005 km^{-1} (**k** has the same direction as $\mathbf{V_p}$), phase speed $V_p = \lambda f$ = 372.9 km/s, and the angle between **k** and magnetic field $\Psi = \cos^{-1}(\mathbf{n_{v_p}} \cdot \mathbf{b})$ = 71.5°. During the period, the four spacecraft had a separation distance of 15.8 – 19.3 km and travelled at a speed of 2.0 km/s. The DIS plasma bulk flow speed is ~30 km/s, much smaller than V_p. This preliminary analysis suggests the validity of the assumption of the temporal stationarity and spatial homogeneity of the MMS plasma data.

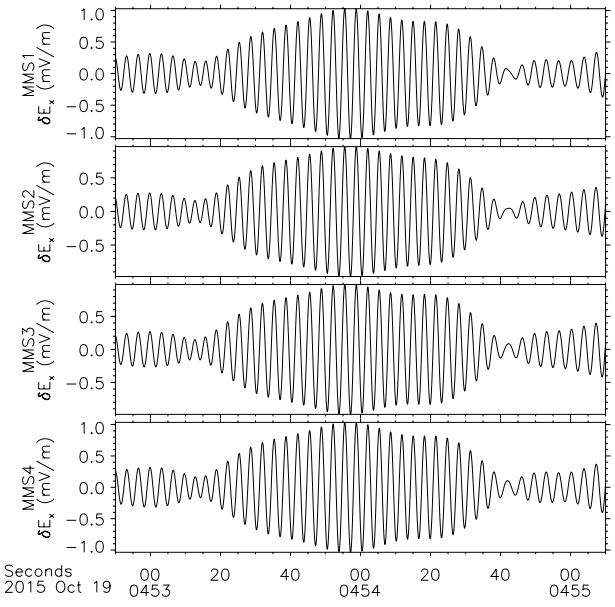

Figure 8. Wave electric field forms on four MMS spacecraft during 0452:50 – 0455:10 UT, 19 October 2015. From top to bottom, the panels show wave electric field component δE_x on MMS1, MMS2, MMS3, and MMS4. The data are transferred into the local field-aligned coordinate system: Z is along the magnetic field, Y=Z×X_{GSE}, and X =Y×Z, which completes the right-hand system.

IV. Conclusions and Future Work

Using MMS field and plasma measurements, we performed a case study of EMIC waves and associated local plasma conditions observed on 19 October 2015. It is suggested that the long-lasting EMIC waves were excited locally. Short inter-spacecraft distances of the MMS mission make it possible to accurately determine the **k** vector of EMIC waves using the phase difference technique. This study helps us better understand several aspects of EMIC waves, e.g., off-equator source regions and wave propagation path and reflection, which still remain under debate or not well explored. [48, 50, 53, 77] The present investigation also extends EMIC wave studies with observations from the inner magnetosphere (e.g., Van Allen Probes) [4, 54-56] or a polar orbit (e.g., Cluster) [26, 28, 57-59] to the low-latitude outer magnetosphere (MMS).

Future work, following the current study, includes 1) to obtain a dispersion relation of EMIC waves by calculating the wave **k** vector as a function of wave frequency, 2) to examine EMIC wave activity in the global magnetosphere by combing observations from other space missions, e.g., Van Allen Probes, THEMIS, and Cluster, and 3) to extend this case study to a statistical study.

Acknowledgments

This work was supported by the 2017 NASA Marshall Faculty Fellowship Program. Work at UNH was also supported by NASA under grant numbers NNX11AO82G and NNX13AE23G. The authors thank the MMS team for their data and software. N. A. Tsyganenko of University of St.-Petersburg in Russian Federation and H. Korth of JHU/APL provided the Tsyganenko magnetic field model and the IDL/Geopack module for magnetic field tracings to calculate the equatorial He^+ gyrofrequencies. Solar wind plasma/IMF data and the geomagnetic indices were obtained from the GSFC/SPDF OMNIWeb interface at http://omniweb.gsfc.nasa.gov.

References

[1]Tsurutani, B. T., and Smith, E. J. "Two types of magnetospheric ELF chorus and their substorm dependences," *Journal of Geophysical Research-Space Physics* Vol. 82, No. 32, 1977, pp. 5112-5128.
doi: 10.1029/JA082i032p05112

[2]Kennel, C. F., and Petschek, H. E. "Limit on stably trapped particle fluxes," *Journal of Geophysical Research* Vol. 71, No. 1, 1966, pp. 1-&.
doi: 10.1029/JZ071i001p00001

[3]Anderson, B. J., Denton, R. E., Ho, G., Hamilton, D. C., Fuselier, S. A., and Strangeway, R. J. "Observational test of local proton cyclotron instability in the Earth's magnetosphere," *Journal of Geophysical Research-Space Physics* Vol. 101, No. A10, 1996, pp. 21527-21543.
doi: 10.1029/96JA01251

[4]Zhang, J. C., Saikin, A. A., Kistler, L. M., Smith, C. W., Spence, H. E., Mouikis, C. G., Torbert, R. B., Larsen, B. A., Reeves, G. D., Skoug, R. M., Funsten, H. O., Kurth, W. S., Kletzing, C. A., Allen, R. C., and Jordanova, V. K. "Excitation of EMIC waves detected by the Van Allen Probes on 28 April 2013," *Geophysical Research Letters* Vol. 41, No. 12, 2014, pp. 4101-4108.
doi: 10.1002/2014GL060621

[5]Fraser, B. J., and Nguyen, T. S. "Is the plasmapause a preferred source region of electromagnetic ion cyclotron waves in the magnetosphere?," *Journal of Atmospheric and Solar-Terrestrial Physics* Vol. 63, No. 11, 2001, pp. 1225-1247.
doi: 10.1016/S1364-6826(00)00225-X

[6]Loto'aniu, T. M., Fraser, B. J., and Waters, C. L. "Propagation of electromagnetic ion cyclotron wave energy in the magnetosphere," *Journal of Geophysical Research-Space Physics* Vol. 110, No. A07214, 2005.
doi: 10.1029/2004JA010816

[7]Pickett, J. S., Grison, B., Omura, Y., Engebretson, M. J., Dandouras, I., Masson, A., Adrian, M. L., Santolik, O., Decreau, P. M. E., Cornilleau-Wehrlin, N., and Constantinescu, D. "Cluster observations of EMIC triggered emissions in association with Pc1 waves near Earth's plasmapause," *Geophysical Research Letters* Vol. 37, No. L09104, 2010.
doi: 10.1029/2010GL042648

[8]Jordanova, V. K., Farrugia, C. J., Thorne, R. M., Khazanov, G. V., Reeves, G. D., and Thomsen, M. F. "Modeling ring current proton precipitation by electromagnetic ion cyclotron waves during the May 14-16, 1997, storm," *Journal of Geophysical Research-Space Physics* Vol. 106, No. A1, 2001, pp. 7-22.
doi: 10.1029/2000JA002008

[9]Lin, R. L., Zhang, J. C., Allen, R. C., Kistler, L. M., Mouikis, C. G., Gong, J. C., Liu, S. Q., Shi, L. Q., Klecker, B., Sauvaud, J. A., and Dunlop, M. W. "Testing linear theory of EMIC waves in the inner magnetosphere: Cluster observations," *Journal of Geophysical Research-Space Physics* Vol. 119, No. 2, 2014, pp. 1004-1027.
doi: 10.1002/2013JA019541

[10]Allen, R. C., Zhang, J.-C., Kistler, L. M., Spence, H. E., Lin, R.-L., Klecker, B., Dunlop, M. W., Andre, M., and Jordanova, V. K. "A statistical study of EMIC waves observed by Cluster: 2. Associated plasma conditions," *Journal of Geophysical Research-Space Physics* Vol. 121, 2016.

doi: 10.1002/2016JA022541
[11]Criswell, D. R. "Pc 1 micropulsation activity and magnetospheric amplification of 0.2- to 5.0-Hz hydromagnetic waves," *Journal of Geophysical Research* Vol. 74, No. 1, 1969, pp. 205-&.
doi: 10.1029/JA074i001p00205
[12]Thorne, R. M., and Horne, R. B. "Modulation of electromagnetic ion cyclotron instability due to interaction with ring current O+ during magnetic storms," *Journal of Geophysical Research-Space Physics* Vol. 102, No. A7, 1997, pp. 14155-14163.
doi: 10.1029/96JA04019
[13]Anderson, B. J., Erlandson, R. E., and Zanetti, L. J. "A statistical study of Pc 1-2 magnetic pulsations in the equatorial magnetosphere, 1. Equatorial occurrence distributions," *Journal of Geophysical Research-Space Physics* Vol. 97, No. A3, 1992, pp. 3075-3088.
doi: 10.1029/91JA02706
[14]Morley, S. K., Ables, S. T., Sciffer, M. D., and Fraser, B. J. "Multipoint observations of Pc1-2 waves in the afternoon sector," *Journal of Geophysical Research-Space Physics* Vol. 114, No. A09205, 2009, pp. -.
doi: 10.1029/2009JA014162
[15]Sibeck, D. G., Mcentire, R. W., Lui, A. T. Y., Lopez, R. E., and Krimigis, S. M. "Magnetic field drift shell splitting: Cause of unusual dayside particle pitch angle distributions during storms and substorms," *Journal of Geophysical Research-Space Physics* Vol. 92, No. A12, 1987, pp. 13485-13497.
doi: 10.1029/JA092ia12p13485
[16]Takahashi, K., Anderson, B. J., Ohtani, S.-I., Reeves, G. D., Takahashi, S., Sarris, T. E., and Mursula, K. "Drift-shell splitting of energetic ions injected at pseudo-substorm onsets," *Journal of Geophysical Research-Space Physics* Vol. 102, No. A10, 1997, pp. 22117–22130.
doi: 10.1029/97JA01870
[17]Shabansky, V. P. "Some Processes in Magnetosphere," *Space Science Reviews* Vol. 12, No. 3, 1971, pp. 299-418.
doi: 0.1007/Bf00165511
[18]McCollough, J. P., Elkington, S. R., and Baker, D. N. "The role of Shabansky orbits in compression-related electromagnetic ion cyclotron wave growth," *Journal of Geophysical Research-Space Physics* Vol. 117, No. A01208, 2012.
doi: 10.1029/2011JA016948
[19]Anderson, B. J., and Hamilton, D. C. "Electromagnetic ion cyclotron waves stimulated by modest magnetospheric compressions," *Journal of Geophysical Research-Space Physics* Vol. 98, No. A7, 1993, pp. 11369-11382.
doi: 10.1029/93JA00605
[20]Usanova, M. E., Mann, I. R., Rae, I. J., Kale, Z. C., Angelopoulos, V., Bonnell, J. W., Glassmeier, K. H., Auster, H. U., and Singer, H. J. "Multipoint observations of magnetospheric compression-related EMIC Pc1 waves by THEMIS and CARISMA," *Geophysical Research Letters* Vol. 35, No. 17, L17S25, 2008, pp. -.
doi: 10.1029/2008GL034458
[21]Usanova, M. E., Mann, I. R., Kale, Z. C., Rae, I. J., Sydora, R. D., Sandanger, M., Soraas, F., Glassmeier, K. H., Fornacon, K. H., Matsui, H., Puhl-Quinn, P. A., Masson, A., and Vallieres, X. "Conjugate ground and multisatellite observations of compression-related EMIC Pc1 waves and associated proton precipitation," *Journal of Geophysical Research-Space Physics* Vol. 115, No. A07208, 2010, pp. -.
doi: 10.1029/2009JA014935
[22]Winglee, R. M., Chua, D., Brittnacher, M., Parks, G. K., and Lu, G. "Global impact of ionospheric outflows on the dynamics of the magnetosphere and cross-polar cap potential," *Journal of Geophysical Research-Space Physics* Vol. 107, No. 1237, 2002.
doi: 10.1029/2001JA000214
[23]McCollough, J. P., Elkington, S. R., Usanova, M. E., Mann, I. R., Baker, D. N., and Kale, Z. C. "Physical mechanisms of compressional EMIC wave growth," *Journal of Geophysical Research-Space Physics* Vol. 115, No. A10214, 2010.
doi: 10.1029/2010JA015393
[24]Liu, Y. H., Fraser, B. J., and Menk, F. W. "Pc2 EMIC waves generated high off the equator in the dayside outer magnetosphere," *Geophysical Research Letters* Vol. 39, No. L17102, 2012.
doi: 10.1029/2012GL053082
[25]Liu, Y. H., Fraser, B. J., Menk, F. W., Zhang, J.-C., Kistler, L. M., and Dandouras, I. "Correction to "Pc2 EMIC waves generated high off the equator in the dayside outer magnetosphere"," *Geophysical Research Letters* Vol. 40, 2013, pp. 1950-1951.
doi: 10.1002/grl.50283
[26]Allen, R. C., Zhang, J.-C., Kistler, L. M., Spence, H. E., Lin, R.-L., Dunlop, M. W., and Andre, M. "Multiple bidirectional EMIC waves observed by Cluster at middle magnetic latitudes in the dayside magnetosphere," *Journal of Geophysical Research-Space Physics* Vol. 118, No. 10, 2013, pp. 6266-6278.
doi: 10.1002/jgra.50600
[27]Zhang, J.-C., Kistler, L. M., Mouikis, C. G., Dunlop, M. W., Klecker, B., and Sauvaud, J.-A. "A case study of EMIC-wave associated He+ energization in the outer magnetosphere: Cluster and Double Star 1 observations," *Journal of Geophysical Research-Space Physics* Vol. 115, No. A06212, 2010.
doi: 10.1029/2009JA014784
[28]Zhang, J. C., Kistler, L. M., Mouikis, C. G., Klecker, B., Sauvaud, J. A., and Dunlop, M. W. "A statistical study of EMIC wave-associated He+ energization in the outer magnetosphere: Cluster/CODIF observations," *Journal of Geophysical Research-Space Physics* Vol. 116, No. A11201, 2011.

doi: 10.1029/2011JA016690

[29]Young, D. T., Perraut, S., Roux, A., Devilledary, C., Gendrin, R., Korth, A., Kremser, G., and Jones, D. "Wave-particle interactions near ΩHe+ observed on GEOS 1 and 2, 1. Propagation of ion cyclotron waves in He+-rich plasma," *Journal of Geophysical Research-Space Physics* Vol. 86, No. A8, 1981, pp. 6755-6772.
doi: 10.1029/JA086iA08p06755

[30]Zhang, J., Halford, A. J., Saikin, A. A., Huang, C.-L., Spence, H. E., Larsen, B. A., Reeves, G. D., Millan, R. M., Smith, C. W., Torbert, R. B., Kurth, W. S., Kletzing, C. A., Blake, J. B., Fennel, J. F., and Baker, D. N. "EMIC waves and associated relativistic electron precipitation on 25–26 January 2013," *Journal of Geophysical Research: Space Physics*, 2016, pp. n/a-n/a.
doi: 10.1002/2016JA022918

[31]Gendrin, R., and Roux, A. "Energization of helium ions by proton-induced hydromagnetic-waves," *Journal of Geophysical Research-Space Physics* Vol. 85, No. A9, 1980, pp. 4577-4586.
doi: 10.1029/JA085iA09p04577

[32]Fuselier, S. A., and Anderson, B. J. "Low-energy He+ and H+ distributions and proton cyclotron waves in the afternoon equatorial magnetosphere," *Journal of Geophysical Research-Space Physics* Vol. 101, No. A6, 1996, pp. 13255-13265.
doi: 10.1029/96JA00292

[33]Jordanova, V. K., Farrugia, C. J., Quinn, J. M., Thorne, R. M., Ogilvie, K. W., Lepping, R. P., Lu, G., Lazarus, A. J., Thomsen, M. F., and Belian, R. D. "Effect of wave-particle interactions on ring current evolution for January 10-11, 1997: Initial results," *Geophysical Research Letters* Vol. 25, No. 15, 1998, pp. 2971-2974.
doi: 10.1029/98GL00649

[34]Fok, M. C., Kozyra, J. U., Nagy, A. F., Rasmussen, C. E., and Khazanov, G. V. "Decay of equatorial ring current ions and associated aeronomical consequences," *Journal of Geophysical Research-Space Physics* Vol. 98, No. A11, 1993, pp. 19381-19393.
doi: 10.1029/93JA01848

[35]Kozyra, J. U., Fok, M. C., Sanchez, E. R., Evans, D. S., Hamilton, D. C., and Nagy, A. F. "The role of precipitation losses in producing the rapid early recovery phase of the Great Magnetic Storm of February 1986," *Journal of Geophysical Research-Space Physics* Vol. 103, No. A4, 1998, pp. 6801-6814.
doi: 10.1029/97JA03330

[36]Thorne, R. M., and Kennel, C. F. "Relativistic electron precipitation during magnetic storm main phase," *Journal of Geophysical Research* Vol. 76, No. 19, 1971, pp. 4446-&.
doi: 10.1029/JA076i019p04446

[37]Jordanova, V. K., Albert, J., and Miyoshi, Y. "Relativistic electron precipitation by EMIC waves from self-consistent global simulations," *Journal of Geophysical Research-Space Physics* Vol. 113, No. A00A10, 2008.
doi: 10.1029/2008JA013239

[38]Loto'aniu, T. M., Thorne, R. M., Fraser, B. J., and Summers, D. "Estimating relativistic electron pitch angle scattering rates using properties of the electromagnetic ion cyclotron wave spectrum," *Journal of Geophysical Research-Space Physics* Vol. 111, No. A04220, 2006.
doi: 10.1029/2005JA011452

[39]Summers, D., and Thorne, R. M. "Relativistic electron pitch-angle scattering by electromagnetic ion cyclotron waves during geomagnetic storms," *Journal of Geophysical Research-Space Physics* Vol. 108, No. A4, 1143, 2003, pp. -.
doi: 10.1029/2002JA009489

[40]Meredith, N. P., Thorne, R. M., Horne, R. B., Summers, D., Fraser, B. J., and Anderson, R. R. "Statistical analysis of relativistic electron energies for cyclotron resonance with EMIC waves observed on CRRES," *Journal of Geophysical Research-Space Physics* Vol. 108, No. A6, 1250, 2003, pp. -.
doi: 10.1029/2002JA009700

[41]Miyoshi, Y., Sakaguchi, K., Shiokawa, K., Evans, D., Albert, J., Connors, M., and Jordanova, V. "Precipitation of radiation belt electrons by EMIC waves, observed from ground and space," *Geophysical Research Letters* Vol. 35, No. L23101, 2008.
doi: 10.1029/2008GL035727

[42]Rodger, C. J., Raita, T., Clilverd, M. A., Seppala, A., Dietrich, S., Thomson, N. R., and Ulich, T. "Observations of relativistic electron precipitation from the radiation belts driven by EMIC waves," *Geophysical Research Letters* Vol. 35, No. L16106, 2008.
doi: 10.1029/2008GL034804

[43]Blum, L. W., Schiller, Q., Li, X., Millan, R., Halford, A., and Woodger, L. "New conjunctive CubeSat and balloon measurements to quantify rapid energetic electron precipitation," *Geophysical Research Letters* Vol. 40, No. 22, 2013, pp. 5833-5837.
doi: 10.1002/2013GL058546

[44]Li, Z., Millan, R. M., and Hudson, M. K. "Simulation of the energy distribution of relativistic electron precipitation caused by quasi-linear interactions with EMIC waves," *Journal of Geophysical Research-Space Physics* Vol. 118, No. 12, 2013, pp. 7576-7583.
doi: 10.1002/2013JA019163

[45]Li, Z., Millan, R. M., Hudson, M. K., Woodger, L. A., Smith, D. M., Chen, Y., Friedel, R., Rodriguez, J. V., Engebretson, M. J., Goldstein, J., Fennell, J. F., and Spence, H. E. "Investigation of EMIC wave scattering as the cause for the BARREL 17 January 2013 relativistic electron precipitation event: A quantitative comparison of simulation with observations," *Geophysical Research Letters* Vol. 41, No. 24, 2014, pp. 8722-8729.
doi: 10.1002/2014GL062273

[46]Hendry, A. T., Rodger, C. J., Clilverd, M. A., Engebretson, M. J., Mann, I. R., Lessard, M. R., Raita, T., and Milling, D. K. "Confirmation of EMIC wave-driven relativisticelectron precipitation," *J. Geophys.Res. Space Physics* Vol. 121, 2016.
doi: 10.1002/2015JA022224

[47]Rodger, C. J., Hendry, A. T., Clilverd, M. A., Kletzing, C. A., Brundell, J. B., and Reeves, G. D. "High-resolution in situ observations of electron precipitation-causing EMIC waves," *Geophysical Research Letters* Vol. 42, No. 22, 2015, pp. 9633-9641.
doi: 10.1002/2015gl066581

[48]Khazanov, G. V., Gamayunov, K. V., Gallagher, D. L., and Kozyra, J. U. "Reply to comment by R. M. Thorne and R. B. Horne Khazanov et al. [2002] and Khazanov et al. [2006]," *Journal of Geophysical Research-Space Physics* Vol. 112, No. A12215, 2007.
doi: 10.1029/2007JA012463

[49]Rauch, J. L., and Roux, A. "Ray tracing of ULF waves in a multicomponent magnetospheric plasma: Consequences for the generation mechanism of ion cyclotron waves," *Journal of Geophysical Research-Space Physics* Vol. 87, No. A10, 1982, pp. 8191-8198.
doi: 10.1029/JA087iA10p08191

[50]Khazanov, G. V., Gamayunov, K. V., Gallagher, D. L., and Kozyra, J. U. "Self-consistent model of magnetospheric ring current and propagating electromagnetic ion cyclotron waves: Waves in multi-ion magnetosphere," *Journal of Geophysical Research-Space Physics* Vol. 111, No. A10202, 2006.
doi: 10.1029/2006JA011833

[51]Horne, R. B., and Thorne, R. M. "On the preferred source location for the convective amplification of ion cyclotron waves," *Journal of Geophysical Research-Space Physics* Vol. 98, No. A6, 1993, pp. 9233-9247.
doi: 10.1029/92JA02972

[52]Horne, R. B., and Thorne, R. M. "Wave heating of He+ by electromagnetic ion cyclotron waves in the magnetosphere: Heating near the H+-He+ bi-ion resonance frequency," *Journal of Geophysical Research-Space Physics* Vol. 102, No. A6, 1997, pp. 11457-11471.
doi: 10.1029/97JA00749

[53]Thorne, R. M., and Horne, R. B. "Comment on Khazanov et al. [2002] and Khazanov et al. [2006]," *Journal of Geophysical Research-Space Physics* Vol. 112, No. A12214, 2007.
doi: 10.1029/2007JA012268

[54]Saikin, A. A., Zhang, J. C., Allen, R. C., Smith, C. W., Kistler, L. M., Spence, H. E., Torbert, R. B., Kletzing, C. A., and Jordanova, V. K. "The occurrence and wave properties of H+-, He+-, and O+-band EMIC waves observed by the Van Allen Probes," *Journal of Geophysical Research-Space Physics* Vol. 120, No. 9, 2015, pp. 7477-7492.
doi: 10.1002/2015JA021358

[55]Saikin, A. A., Zhang, J. C., Smith, C. W., Spence, H. E., Torbert, R. B., and Kletzing, C. A. "The dependence on geomagnetic conditions and solar wind dynamic pressure of the spatial distributions of EMIC waves observed by the Van Allen Probes," *Journal of Geophysical Research: Space Physics* Vol. 121, No. 5, 2016, pp. 4362-4377.
doi: 10.1002/2016JA022523

[56]Zhang, J. C., Halford, A. J., Saikin, A. A., Huang, C. L., Spence, H. E., Larsen, B. A., Reeves, G. D., Millan, R. M., Smith, C. W., Torbert, R. B., Kurth, W. S., Kletzing, C. A., Blake, J. B., Fennel, J. F., and Baker, D. N. "EMIC waves and associated relativistic electron precipitation on 25-26 January 2013," *Journal of Geophysical Research-Space Physics* Vol. 121, No. 11, 2016, pp. 11086-11100.
doi: 10.1002/2016ja022918

[57]Allen, R. C., Zhang, J. C., Kistler, L. M., Spence, H. E., Lin, R. L., Klecker, B., Dunlop, M. W., André, M., and Jordanova, V. K. "A statistical study of EMIC waves observed by Cluster: 1. Wave properties," *Journal of Geophysical Research: Space Physics* Vol. 120, No. 7, 2015, pp. 5574-5592.
doi: 10.1002/2015JA021333

[58]Allen, R. C., Zhang, J. C., Kistler, L. M., Spence, H. E., Lin, R. L., Klecker, B., Dunlop, M. W., André, M., and Jordanova, V. K. "A statistical study of EMIC waves observed by Cluster: 2. Associated plasma conditions," *Journal of Geophysical Research: Space Physics* Vol. 121, No. 7, 2016, pp. 6458-6479.
doi: 10.1002/2016JA022541

[59]Zhang, J. C., Kistler, L. M., Mouikis, C. G., Dunlop, M. W., Klecker, B., and Sauvaud, J. A. "A case study of EMIC wave-associated He plus energization in the outer magnetosphere: Cluster and Double Star 1 observations," *Journal of Geophysical Research-Space Physics* Vol. 115, No. A06212, 2010.
doi: 10.1029/2009JA014784

[60]Burch, J. L., Moore, T. E., Torbert, R. B., and Giles, B. L. "Magnetospheric Multiscale Overview and Science Objectives," *Space Science Reviews* Vol. 199, No. 1-4, 2016, pp. 5-21.
doi: 10.1007/s11214-015-0164-9

[61]Russell, C. T., Anderson, B. J., Baumjohann, W., Bromund, K. R., Dearborn, D., Fischer, D., Le, G., Leinweber, H. K., Leneman, D., Magnes, W., Means, J. D., Moldwin, M. B., Nakamura, R., Pierce, D., Plaschke, F., Rowe, K. M., Slavin, J. A., Strangeway, R. J., Torbert, R., Hagen, C., Jernej, I., Valavanoglou, A., and Richter, I. "The Magnetospheric Multiscale Magnetometers," *Space Science Reviews* Vol. 199, No. 1-4, 2016, pp. 189-256.
doi: 10.1007/s11214-014-0057-3

[62]Torbert, R. B., Russell, C. T., Magnes, W., Ergun, R. E., Lindqvist, P. A., LeContel, O., Vaith, H., Macri, J., Myers, S., Rau, D., Needell, J., King, B., Granoff, M., Chutter, M., Dors, I., Olsson, G., Khotyaintsev, Y. V., Eriksson, A., Kletzing, C. A., Bounds, S., Anderson, B., Baumjohann, W., Steller, M., Bromund, K., Le, G., Nakamura, R., Strangeway, R. J., Leinweber, H. K., Tucker, S., Westfall, J., Fischer, D., Plaschke, F., Porter, J., and Lappalainen, K. "The FIELDS Instrument Suite on MMS: Scientific Objectives, Measurements, and Data Products," *Space Science Reviews* Vol. 199, No. 1-4, 2016, pp. 105-135.
doi: 10.1007/s11214-014-0109-8

[63]Pollock, C., Moore, T., Jacques, A., Burch, J., Gliese, U., Saito, Y., Omoto, T., Avanov, L., Barrie, A., Coffey, V., Dorelli, J., Gershman, D., Giles, B., Rosnack, T., Salo, C., Yokota, S., Adrian, M., Aoustin, C., Auletti, C., Aung, S., Bigio, V., Cao, N., Chandler, M., Chornay, D., Christian, K., Clark, G., Collinson, G., Corris, T., De Los Santos, A., Devlin, R., Diaz, T., Dickerson, T., Dickson, C., Diekmann, A., Diggs, F., Duncan, C., Figueroa-Vinas, A., Firman, C., Freeman, M., Galassi, N., Garcia, K., Goodhart, G., Guererro, D., Hageman, J., Hanley, J., Hemminger, E., Holland, M., Hutchins, M., James, T., Jones, W., Kreisler, S., Kujawski, J., Lavu, V., Lobell, J., LeCompte, E., Lukemire, A., MacDonald, E., Mariano, A., Mukai, T., Narayanan, K., Nguyan, Q., Onizuka, M., Paterson, W., Persyn, S., Piepgrass, B., Cheney, F., Rager, A., Raghuram, T., Ramil, A., Reichenthal, L., Rodriguez, H., Rouzaud, J., Rucker, A., Saito, Y., Samara, M., Sauvaud, J. A., Schuster, D., Shappirio, M., Shelton, K., Sher, D., Smith, D., Smith, K., Smith, S., Steinfeld, D., Szymkiewicz, R., Tanimoto, K., Taylor, J., Tucker, C., Tull, K., Uhl, A., Vloet, J., Walpole, P., Weidner, S., White, D., Winkert, G., Yeh, P. S., and Zeuch, M. "Fast Plasma Investigation for Magnetospheric Multiscale," *Space Science Reviews* Vol. 199, No. 1-4, 2016, pp. 331-406.
doi: 10.1007/s11214-016-0245-4

[64]Young, D. T., Burch, J. L., Gomez, R. G., De Los Santos, A., Miller, G. P., Wilson, P., Paschalidis, N., Fuselier, S. A., Pickens, K., Hertzberg, E., Pollock, C. J., Scherrer, J., Wood, P. B., Donald, E. T., Aaron, D., Furman, J., George, D., Gurnee, R. S., Hourani, R. S., Jacques, A., Johnson, T., Orr, T., Pan, K. S., Persyn, S., Pope, S., Roberts, J., Stokes, M. R., Trattner, K. J., and Webster, J. M. "Hot Plasma Composition Analyzer for the Magnetospheric Multiscale Mission," *Space Science Reviews* Vol. 199, No. 1-4, 2016, pp. 407-470.
doi: 10.1007/s11214-014-0119-6

[65]Anderson, B. J., Denton, R. E., and Fuselier, S. A. "On determining polarization characteristics of ion cyclotron wave magnetic field fluctuations," *Journal of Geophysical Research-Space Physics* Vol. 101, No. A6, 1996, pp. 13195-13213.
doi: 10.1029/96JA00633

[66]O'Brien, T. P., and McPherron, R. L. "An empirical phase space analysis of ring current dynamics: Solar wind control of injection and decay," *Journal of Geophysical Research-Space Physics* Vol. 105, No. A4, 2000, pp. 7707-7719.
doi: 10.1029/1998JA000437

[67]Weimer, D. R. "Correction to "Predicting interplanetary magnetic field (IMF) propagation delay times using the minimum variance technique"," *Journal of Geophysical Research-Space Physics* Vol. 109, No. A12104, 2004, p. 1.
doi: 10.1029/2004JA010691

[68]Weimer, D. R., and King, J. H. "Improved calculations of interplanetary magnetic field phase front angles and propagation time delays," *Journal of Geophysical Research-Space Physics* Vol. 113, No. A01105, 2008, p. 14.
doi: 10.1029/2007JA012452

[69]Weimer, D. R., Ober, D. M., Maynard, N. C., Collier, M. R., McComas, D. J., Ness, N. F., Smith, C. W., and Watermann, J. "Predicting interplanetary magnetic field (IMF) propagation delay times using the minimum variance technique," *Journal of Geophysical Research-Space Physics* Vol. 108, No. A1, 2003, p. 12.
doi: 10.1029/2002JA009405

[70]Gary, S. P., Moldwin, M. B., Thomsen, M. F., Winske, D., and McComas, D. J. "Hot proton anisotropies and cool proton temperatures in the outer magnetosphere," *Journal of Geophysical Research-Space Physics* Vol. 99, No. A12, 1994, pp. 23603-23615.
doi: 10.1029/94JA02069

[71]Blum, L. W., MacDonald, E. A., Gary, S. P., Thomsen, M. F., and Spence, H. E. "Ion observations from geosynchronous orbit as a proxy for ion cyclotron wave growth during storm times," *Journal of Geophysical Research-Space Physics* Vol. 114, No. A10214, 2009.
doi: 10.1029/2009JA014396

[72]Chanteur, G. "Spatial interpolation for four spacecraft: Theory," *Analysis Methods for Multi-Spacecraft Data*. Vol. SR-001 (Electronic edition 1.1), ESA Publications Division, 2000, pp. 349-370.

[73]Pinçon, J. L., and Lefeuvre, F. "Local characterization of homogeneous turbulence in a space plasma from simultaneous measurements of field components at several points in space," *Journal of Geophysical Research-Space Physics* Vol. 96, No. A2, 1991, pp. 1789-1802.
doi: 10.1029/90JA02183

[74]Motschmann, U., Woodward, T. I., Glassmeier, K. H., Southwood, D. J., and Pincon, J. L. "Wavelength and direction filtering by magnetic measurements at satellite arrays: Generalized minimum variance analysis," *Journal of Geophysical Research-Space Physics* Vol. 101, No. A3, 1996, pp. 4961-4965.
doi: 10.1029/95JA03471

[75]Neubauer, F. M., and Glassmeier, K. H. "Use of an array of satellites as a wave telescope," *Journal of Geophysical Research-Space Physics* Vol. 95, No. A11, 1990, pp. 19115-19122.
doi: 10.1029/JA095iA11p19115

[76]Glassmeier, K. H., Motschmann, U., Dunlop, M., Balogh, A., Acuna, M. H., Carr, C., Musmann, G., Fornacon, K. H., Schweda, K., Vogt, J., Georgescu, E., and Buchert, S. "Cluster as a wave telescope - first results from the fluxgate magnetometer," *Annales Geophysicae* Vol. 19, No. 10-12, 2001, pp. 1439-1447.
doi: 10.5194/angeo-19-1439-2001

[77]Khazanov, G. V., Gamayunov, K. V., Jordanova, V. K., and Krivorutsky, E. N. "A self-consistent model of the interacting ring current ions and electromagnetic ion cyclotron waves, initial results: Waves and precipitating fluxes," *Journal of Geophysical Research-Space Physics* Vol. 107, No. A6, 2002.
doi: 10.1029/2001JA000180